# Antimicrobial Activity of Iron-Halide Complexes Against Gram-Positive and Gram-Negative Bacteria

Nusrat Abedin[a‡], Abdullah Hamed A Alshehri[a], Ali M A Almughrbi[a], Olivia Moore[a], Sheikh Alyza[a], Elizabeth K. Rusbridge[a], Naqash Masood[b], Biola F. Egbowon[a], Alan J. Hargreaves[a], Anthony J. Fitzpatrick[a]* and Felix Dafhnis-Calas[c]*

a. School of Science and Technology, Nottingham Trent University, Clifton Lane, Nottingham NG11 8NS, UK.

email: anthony.fitzpatrick@ntu.ac.uk

b. School of Life Sciences, Keele University, Keele, Staffordshire, ST5 5BG, UK.

c. School of Life Sciences, Queens Medical Centre, University of Nottingham, NG7 2UH, UK

email: felix.Dafhnis-calas@nottingham.ac.uk

‡ Current Address: Institute of Food Science and Technology (IFST), Bangladesh Council of Scientific and Industrial Research (BCSIR), Dr Qudrat-I-Khuda Road, Dhanmondi, Dhaka 1205, Bangladesh.

**Abstract**

Antimicrobial resistance (AMR) has become one of the more serious threats to the global health. The emergence of bacteria resistant to antimicrobial substances decreases the potencies of current antibiotics. Consequently, there is an urgent and growing need for the developing of new classes of antibiotics. Three prepared novel iron complexes have a broad-spectrum antimicrobial activity with minimum bactericidal concentration (MBC) values ranging from 3.5 to 10 mM and 3.5 to 40 mM against Gram-positive and Gram-negative bacteria with antimicrobial resistance phenotype, respectively. Time-kill studies and quantification of the extracellular DNA confirmed the bacteriolytic mode of action of the iron-halide compounds. Additionally, the novel complexes showed significant antibiofilm activity against the tested pathogenic bacterial strains at concentrations lower than the MBC. The cytotoxic effect of the complexes on different mammalian cell lines show sub-cytotoxic values at concentrations lower than the minimum bactericidal concentrations.

## Introduction

Antimicrobial resistance (AMR) has become a serious threat to global health.[1,2] The mortality rate and economic burden of infections caused by antimicrobial-resistant pathogens are increasing. Diseases caused by antimicrobial-resistant bacteria are currently claiming 50,000 lives each year across Europe and the USA with 100,000 more deaths in other areas of the world. Furthermore, it is estimated that antibiotic resistance will cause around 300 million premature deaths by 2050, with a loss of up to $100 trillion to the global economy.[3] The combination of this growing antibiotic resistance, paired with the declining antibiotic pipeline, has led to the rise of infectious diseases that are almost untreatable.[4–6]

Recently, the World Health Organization (WHO) published a list of antibiotic-resistant pathogens that pose a major threat to human health. The most critical groups include pathogens such as *Acinetobacter baumannii*, *Pseudomonas aeruginosa*, *Enterobacteriaceae, Staphylococcus aureus* and *Campylobacter spp.* For instance, methicillin resistant *Staphylococcus aureus* (MRSA), a leading cause in hospital-acquired infections, is one of the most common and deadly causes of AMR. Current studies estimate that patients with MRSA are 60% more likely to die than patients with infections by methicillin sensitive *Staphylococcus aureus* (MSSA).

In addition to antibiotic-resistant *S. aureus*, infections caused by multidrug-resistant Gram-negative bacteria have dramatically increased worldwide. Gram-negative bacteria are the most common cause of hospital acquired infection, as well as the leading cause of infection in the intensive care unit (ICU).[7] The infections produced by multidrug-resistant bacteria (MDR) result in significantly higher mortality when compared to those caused by non-antibiotic resistant strains. In the United States, Gram-negative bacteria are responsible for 30% of the nosocomial infections and 70% of the intensive care unit infections.[8–10] All together, these factors demonstrate that there is an urgent need for the development of novel antimicrobial agents that have a broad-spectrum of activity and can be efficaciously used against antibiotic-resistant bacteria.[3,11]

Recently, there has been an increase in research studies that target the discovery of antimicrobial compounds with mechanisms of action unknown to the pathogenic bacteria. For instance, several groups have explored the antibacterial activity of various metal complexes.[12–17] These studies explored the antimicrobial activity of novel metal complexes formed by coordinating various metal ions to known antibiotics. The novel interaction between the metal ion and the organic compound showed higher antimicrobial activity than the free ligands. This improved antimicrobial property highlighted significant differences between the mechanisms of action of the metal complex and its free ligands.[18,19] This result, and other recent reports, indicate that the study of the antimicrobial activity of novel metal-complexes could lead to the discovery of antibiotics with novel mechanisms of action to combat those bacteria with resistant phenotypes. The potential antibiotic use of the metal-complexes is also strengthened by those reports showing metal-derived compounds with effective antimicrobial or antifungal activity, while not displaying any cytotoxicity against mammalian cell lines.[20,21]

Herein, we address this challenge by evaluating the antimicrobial activity of three novel iron-halide complexes. Complex 1 comprises a previously reported Fe(II) complex, $[Fe(Hampy)_2Cl_4]$, with an equatorially coordinating tetrachloride motif balanced by aminopyrazinium (Hampy) ligands in the axial positions.[22] Complex 2 is the tetrabromide analogue, $[Fe(Hampy)_2Br_4]$, newly synthesised for this investigation. Complex 3 is an Fe(III) complex, $[Fe(bipy)(Sal)Cl_2]$, related to **1** and **2** through the synthesis method, based on a coordinating bipyrdine, salicylaldehyde and two chloride ligands **(Fig 1)**. The main objective of this study was to evaluate and compare the antibacterial activity of these iron-halide complexes. Furthermore, the cytotoxic effect of the iron complexes against different mammalian cell lines was assessed.

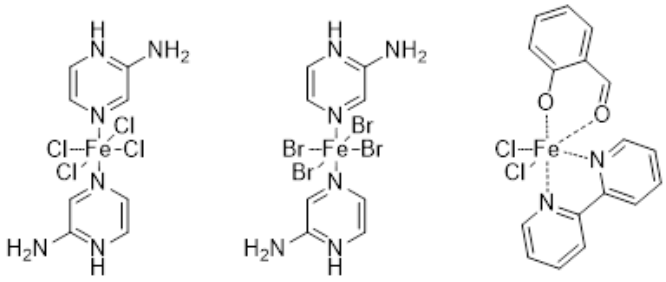

Figure 1. Structure of the iron-halide complexes **1**, **2**, and **3.**

# Experimental

**Synthesis of the Fe halide complexes**

Synthesis of Complex **(1),** $[Fe(Hampy)_2Cl_4]$, was performed according to our previous work.[22]
Synthesis of Complex **(2),** $[Fe(Hampy)_2Br_4]$,was adapted from complex **(1)**. 0.095 g (1 mmol) of 2-aminopyrazine was first added to 0.105 ml (1 mmol) of salicylaldehyde in 15 ml of 1:1 methanol:acetonitrile. Ferric bromide (0.400 g) was added to the solution, initially resulting in a red colour, which later became dark purple. This mixture was then filtered after a further 10 min of stirring. Upon evaporation of the solvent, dark purple crystals were isolated and washed in acetone, yield: 0.1839 g, 32 %. IR: υmax (neat) / cm-1 3306, 3088, 1649, 1620, 770, 706. Elemental, Theory (Found): C 16.19(16.23), H 1.78(1.84), N 14.86(14.88).

For the synthesis of complex **(3),** $[Fe(bipy)(Sal)Cl_2]\cdot CH_3CN$, 2-aminopyrazine (1 mmol, 0.095 g) was added to salicylaldehyde (1 mmol, 0.122 g) in 1:1 methanol/acetonitrile (15 mL) and stirred for 10 min. Ferric chloride hydrate (2 mmol, 0.541 g) was then added to this solution, resulting in a dark red colour immediately followed by the addition of 2,2´-bipyridyl (0.156 g 1 mmol). The solution was filtered after 20 min stirring and small, dark red plate-like crystals formed after several days of slow solvent evaporation. Yield: 0.2589 g. IR: υmax (neat) / $cm^{-1}$ 3304, 3051, 1655, 1620, 773, 678. Elemental, Theory (Found): C 51.27(50.95), H 3.62(3.39), N 9.44(7.55).

**Bacteria strains and growth conditions**

The bacteria strains used in these studies were the methicillin resistant *Staphylococcus aureus NCTC 12493*, *Pseudomonas aeruginosa* strain, *PAO1* and *Escherichia coli NCTC 10418*. Unless otherwise indicated, the bacteria strains were grown in Muller Hinton broth (MHB) or MHB containing 3% agar (MHA). All the cultures were incubated at 37°C for 16 hours.

**Disk diffusion assay**

The antibiotic susceptibility test of six commonly used antibiotics was carried out using the disc diffusion assay on Muller-Hinton agar against the *S. aureus*, *P. aeruginosa* and *E. coli* strains. The list and the potency of antibiotics per disc are as follows; Cefalexin (30µg/disc), Erythromycin (5 µg/disc), Ciprofloxacin (5 µg/disc), Rifampicin (2 µg/disc), Vancomycin (5 µg/disc), Bacitracin (10 µg/disc), Gentamicin (10 µg/disc), Imipenem (10 µg/disc). The assay was performed and evaluated according to the Clinical and Laboratory Standards Institute (CLSI) guidelines.[23]

**Well diffusion assay**

Stock solutions (36 mg/mL) of the iron (II) complexes were prepared in $H_2O$. The inoculum suspensions of test bacteria strains were prepared from overnight broth cultures and the turbidity equivalent adjusted to 0.5 McFarland standard, which gave a concentration of $1.0 \times 10^8$ bacterial cells/ml. Then, freshly prepared MHA plates were seeded with 100 µL broth culture. Thereafter, 6 mm diameter wells were made on the agar surface before loading the well with 50 µL of each compound dissolved in $H_2O$. Plates inoculated with each test bacterium were incubated at 37°C for 16 h. After incubation, the diameters of the inhibition zones formed on the MHA plates were determined in millimetres. Rifampicin (2 µg/disc) and imipenem (10 µg/disc) were used as a positive control for Gram-positive and Gram-negative respectively.

**Agar dilution test**

The assay was performed and evaluated according to the Clinical and Laboratory Standards Institute (CLSI) guidelines.[23] The bacterial cultures were prepared in 5 ml of MHB following by incubation at 37°C for 16-18h. The bacterial cells were collected by centrifugation at 1344 × g for 5 min and suspended in sterile distilled water. The turbidity was adjusted to 0.5 McFarland standard, giving a cell density of ~ $1\times10^8$ CFU/ml. The cell suspension was diluted by a factor of 10 and 1 µl of this diluted culture was spotted onto the MHA plates containing different concentrations of the iron-halide complexes. The MHA containing the antimicrobial compounds were prepared by

mixing 1 ml of the melted MHA with 1ml of the iron compound dissolved in MHB. Next, two-fold serial dilutions of the compounds dissolved in the agar solution were prepared and poured into different plates. Two control experiments containing no iron-complexes were also prepared; one was used to assess the sterility of the medium and the other was used as a bacterial growth control. The tests were performed in triplicate and the MBC was defined as the minimum concentration at which no bacterial growth was detected.

**Time-kill experiment**

Time-kill experiments of the iron-halide complexes were carried out against the *MRSA* strain NCTC 12493. The assay was performed and evaluated according to according to the Clinical and Laboratory Standards Institute (CLSI) guidelines. The bacteria were cultured to exponential phase at 37°C in MHB, followed by dilution of the cell suspension to obtain a final inoculum of 5 x $10^5$ CFU/ml. This diluted culture was then exposed to the iron compounds at 1x and 0.5x MBC. The cultures were then incubated at 37°C on an orbital shaker at 120 rpm. Next, samples were removed at different time points (0, 2, 4, 6 and 24 h) and plated on MHA for enumeration of colony forming units (CFU/ml).

**Study of biofilm formation and dispersal**

In the biofilm formation experiment, the MRSA strain was grown overnight at 37˚C in 5 ml LB broth, after which a 1:100 dilution of the overnight culture was prepared in RPMI medium supplemented with 0.5% (w/v) glucose. The diluted bacterial culture was then grown in a 96-well plate, both in the presence and absence of the iron-halide complexes. The tested concentrations of the compounds ranged from 0 to 7 mM. Both treated and untreated cultures were incubated at 37°C for 24 h to allow the formation of an adherent biofilm. The medium was removed, and the adherent cells were washed three time with distilled water before staining with 0.1% (w/v) crystal violet. The plates were then washed with distilled water followed by resuspension of the crystal violet with 300 µL of ethanol/acetone, 80/20%. The absorbance of each well was measured in a spectrophotometer set at 570 nm.
For the biofilm dispersal experiment, a 24 h MRSA biofilm was first washed with distilled water and then exposed to the iron- halide complexes at the indicated concentrations for 24 hours. After 24 h of incubation at 37 ˚C, the medium was removed, and the biofilm was washed three times with distilled water. Subsequent staining of the attached cells with 0.1% (w/v) crystal violet was followed by a washing step and dye resuspension with ethanol/acetone mix. As previously, the absorbance of each well was then measured spectrophotometrically at 570 nm.

**Extracellular DNA quantification**

The DNA released from the antimicrobial-treated bacteria was assessed in an 18 h MH culture (37°C, 200 rpm). After measuring the $OD_{600}$ of the cultures, 1 ml of each was centrifuged and the cell-free supernatant filtered (0.22 µm). Next, a QIAprep DNA mini kit (Qiagen GmbH, Hilden, Germany) was used for purification of extracellular DNA (eDNA). The concentration of eDNA was then measured with a NanoDrop™ spectrophotometer, and values normalized to the corresponding $OD_{600}$. Each measurement was carried out in triplicate for each strain and means were compared with those obtained for the wild type.

**Mammalian cell studies**

**Cell culture**

HaCaT cells (human immortalized keratinocytes) were kindly donated by Dr. M. Ahmed., School of Science and Technology, Nottingham Trent University, and were cultured in Dulbecco's modified Eagle's medium (DMEM) (BE12-604F; Lonza Pharma & Biotech, UK), supplemented with 10% foetal bovine serum (HyClone, HYC85; Scientific Laboratory Supplies, UK), 50 U/mL penicillin and 100 µg/mL streptomycin (LZDE17-602E; Lonza Pharma & Biotech, UK), under standard conditions (37°C, 5% $CO_2$). Cells were sub-cultured in T75 flasks and allowed to grow until they were 90 % confluent when they were passaged.

**Measurement of cell metabolism by methyl blue tetrazolium reduction assay**

Cell viability was measured through the reduction of 3-[4,5-dimethylthiazol-2-yl]-2,5-diphenyltetrazolium bromide (MTT) by cellular dehydrogenases. Cells were plated in 94-well plates (Sarstedt, UK) at 25,000 cells/ml in 0.2 ml growth medium and left for 24 h to recover. The growth medium was carefully aspirated from the wells and replaced with fresh medium containing a range of concentrations (up to 30 mM) of complex 1, 2 and 3, followed by incubation for a further for 24 h. A volume of 20 µl of MTT (5 mg/ml in phosphate buffered saline (PBS: 137 mM NaCl, 2.7 mM KCl, 10 mM $Na_2HPO_4$, 2 mM $KH_2PO_4$) was added to each well prior to the end of the experimental

incubation time, and the cells were incubated for a further 30 min at 37 °C. The growth medium was then carefully aspirated, 0.2 ml DMSO was added to each well and the plates were gently agitated to dissolve the reduced formazan product. The absorbance of the solubilised reduced MTT was then measured in a standard microtiter plate reader at a wavelength of 570 nm. Each concentration was tested in triplicate, while three replicate assays were performed.

**Measurement of cell viability *via* Alamar Blue assay**

Cell viability was also measured in HaCaT cells *via* alamar Blue (AB) assay. AB is a water-soluble dye that has been previously used for quantifying *in vitro* viability of various cells.[24,25] Since it is extremely stable and more importantly non-toxic to the cells, continuous monitoring of cultures over time is possible. Both MTT and AB assays are based on the ability of viable cells to produce formazan from the cleavage of the tetrazolium salt by functional mitochondria.[26] However, the MTT test necessitates killing the cells, while AB does not.
Cells were plated in 96-well flat bottom plates, at 25,000 cells/ml in 0.2 ml growth medium after an initial 24 h period of cell recovery and attachment. Cells were then treated with complex 1, 2 and 3 at doses ranging from 0.08-30 mM for 24 h. The medium was aspirated and replaced with a pre-warmed fresh medium containing AB at a final concentration of 10% and the cells were incubated further for 2 h. Optical density of the plate was measured at 560 and 600 nm with a standard spectrophotometer.

**Assessment of cell proliferation by Trypan Blue dye exclusion assay**

Cell proliferation was measured by Trypan Blue exclusion assay. Briefly, cells were seeded in 96- well plate at a density of 25,000 cells/ml in 0.2 ml growth medium and after 24 h, the wells were treated with complex 1, 2 and 3 at doses ranging from 0.08-30 mM. Cell proliferation was assessed by counting dead cells that were stained with Trypan Blue (0.4% in phosphate-buffered saline, PBS) as previously described.[27] Each concentration was tested in triplicate, while three replicate assays were performed.

**Statistical analyses**

The experiments were performed independently at least three times and results are shown as means, with the standard error of means (S.E.M.) as error bars. Statistical significance of the experimental results (significance level of $p<0.05$) was calculated by one-way ANOVA. The half-maximal inhibitory concentrations ($IC_{50}$) were calculated by a non-linear regression analysis. All the analyses were carried out by using GraphPad Prism software (GraphPad Software, San Diego, CA).

## Results and Discussion

**Structural analysis of complexes 2 and 3**

Complex **2** results from the modified synthesis previously reported for complex **1.** The structural motif is identical to complex **1**. The use of ferric bromide rather than chloride results in an iron (II) species with equatorial bromide ligands balanced by aminopyrazinium ligands in the axial positions (fig 2a). As discussed previously, the complex is the result of a redox couple between the Fe (III) species and the aldehyde used in the synthesis.
Complex **3** results from the competitive addition of a co-ligand to the mixture containing the ferric chloride iron source. The addition of the bipyridine ligand inhibits the redox chemistry and forms a more straightforward Fe (III) complex containing one bidentate coordinated bipyridine, two chloride ligands and finally, one salicylaldehyde coordinated through the aldehyde lone pair and a deprotonated phenolate oxygen, as shown in Fig 2b.

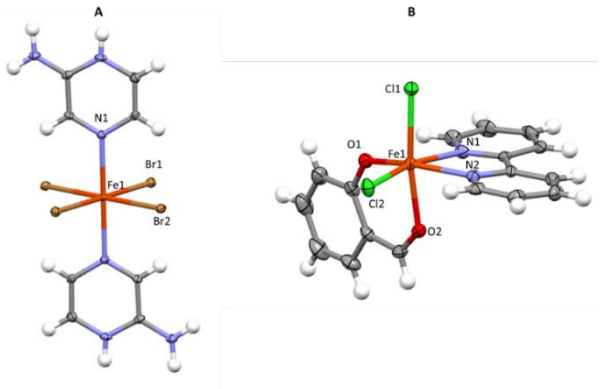

Figure 2**:** A) Structure of complex **2** at 150 K; B) Structure of complex **3** at 150 K, solvent removed for clarity.

Complex **2** is isostructural to the previously published complex **1**. The same hydrogen-halogen bonding 3-D architecture is present throughout the lattice with the hydrogen on the pyrazine nitrogen and the amine interacting with the bromide ligands of neighbouring complexes, Fig 3. Complex **3**, exhibits only small π-π overlap between the bipyridine ligands over neighbouring complexes forming *pseudo*-dimers, Fig 4.

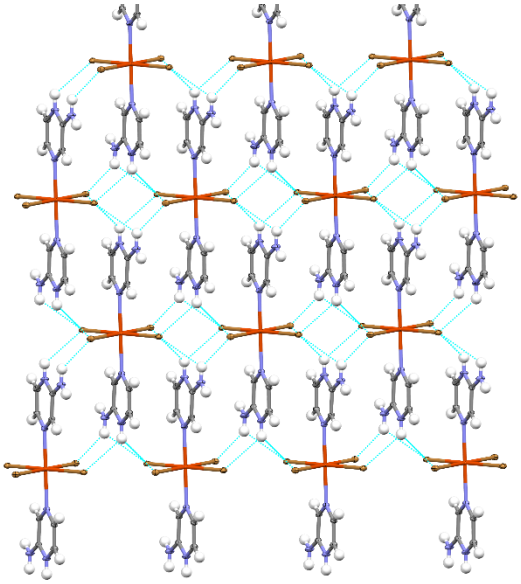

Figure 3: Hydrogen-halogen interactions between neighbouring complexes in complex **2**. Hydrogen bonding in blue.

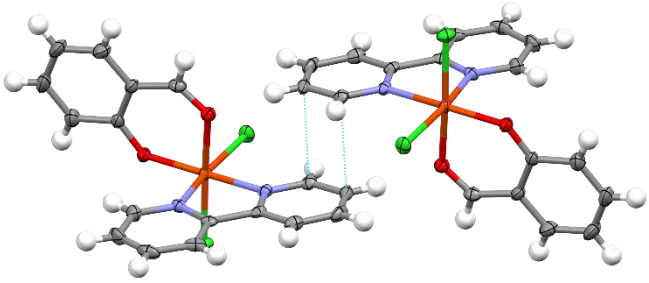

Figure 4: π-π dimers in complex **3**. Hydrogen bonding in blue.

The metal-ligand bond lengths in each complex indicate a high spin ion S = 2 for **2**, S = 5/2 for **3**, Table 1.

Table 1: Bond lengths for complexes **2** and **3** at 150 K.

| Complex **2** | Å | Complex **3** | Å |
|---|---|---|---|
| Fe-N1 | 2.233(3) | Fe-N1 | 2.170(3) |
| Fe-Br1 | 2.6267(9) | Fe-N2 | 2.191(3) |
| Fe-Br2 | 2.6192(9) | Fe-O1 | 1.917(2) |
| | | Fe-O2 | 2.101(2) |
| | | Fe-Cl1 | 2.3117(9) |
| | | Fe-Cl2 | 2.2894(9) |

**Effect of the iron-halide complexes on bacterial cell growth**

Well-diffusion tests, using complexes **1-3,** were performed in order to investigate any possible inhibitory effect on bacterial cell growth. Three independent experiments were carried out against Gram-positive and Gram-negative bacteria; *E. coli* NCTC (10418), MRSA (JCT0031) and the *P. aeruginosa* (PAO1). Previous characterization of these bacterial strains showed their resistance to a wide variety of antibiotics **(Table S1)**. The novel iron complexes were tested against the antibiotic resistance strains *via* well-diffusion test at a final concentration of 40 mM. The results of this experiment indicated that the three iron-halide complexes and their $FeCl_3$ and $FeBr_3$ precursor metal salts inhibited bacterial cell growth **(Fig 5)**. The zones of clearance for most of the strains tested against complex **2** and complex **3** were between 15 and 25 mm. However, the zone of inhibition observed in all experiments using complex **1** were between 12 and 15 mm. There was no significant difference in the susceptibility of Gram-positive and Gram-negative bacteria. In addition, **Figure 5** shows that exposure of the bacteria to the 2-aminopyrazine ligand did not have any negative effect on cell growth.

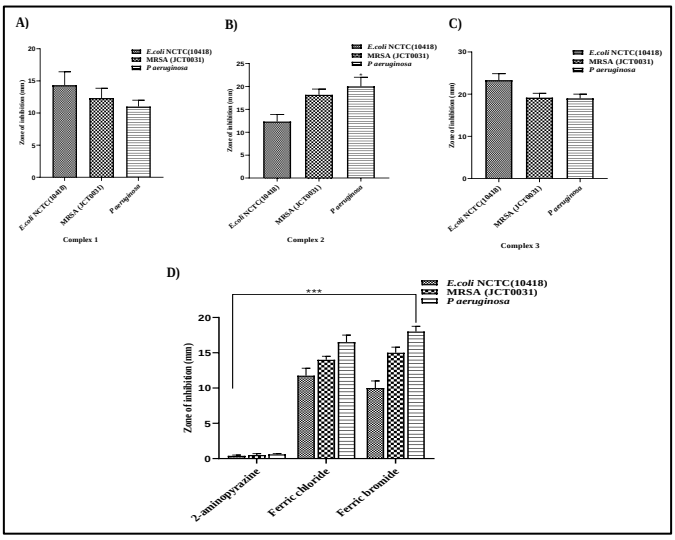


**Figure 5:** Growth inhibition of antibiotic resistance strains for **1-3** as well as their precursor ligands and metal salts. Well-diffusion assays of the **A)** Complex **1**, **B)** Complex **2**, **C)** Complex **3** and **D)** Precursors, were carried out against the *E.coli, P. aeruginosa and MRSA* strains. The differences between all values of zone of inhibition were analysed statistically by using one-way ANOVA test, * P<0.05; *** P<0.001; Error bars indicate the standard error of means; n = 3.

Agar dilution tests were then performed to determine the lowest concentration at which complexes prevented bacterial cell growth. MHA plates containing various concentrations of the iron (II) complexes from 40 mM to 1 mM were prepared, followed by inoculation of those plates with a bacterial cell suspension containing $10^4$ CFU **(Table 2)**. The experimental findings showed that the minimal bactericidal concentration (MBC) of complexes **1** and **2** were 5 mM and 3.5 mM, respectively. However, the MBC value of complex **3** was 10 mM for MRSA and *P. aeruginosa*, whereas in the *E.coli* experiment it was 4-fold higher, at 40 mM.

Interestingly, the MBC of the $FeCl_3$ was higher than the MBC values of its derivative iron (II) complex. In contrast, the MBC of the $FeBr_3$ was lower than the MBC values of complex 2. Similarly, the MBC value of the $FeCl_3$ was lower than the MBCs of complex **3**.

**Table 1**. Minimal bactericidal concentration of the iron-halide complexes and their ligands.

| | Minimal bactericidal concentration (mM) | | | | |
|---|---|---|---|---|---|
| | **1** | **2** | **3** | **FeCl3** | **FeBr3** |
| *MRSA* | 5±0.21 | 3.5±0.01 | 10±0.35 | 24±0.35 | 1.2±0.01 |
| *P. aeruginosa* | 5±0.11 | 3.5±0.21 | 10±0.22 | 12±0.55 | 1.2±0.02 |
| *E. coli* | 5±0.22 | 3.5±0.02 | 40±0.56 | 25±0.22 | 1.2±0.11 |

$5x10^5$ CFU/ml bacteria suspensions were incubated with different concentrations of the iron complexes and their ligands. MBC was defined as the minimal concentration where ≥99.9% bacteria death of initial inoculum was observed. Data represent three independent measurements (means ± SEM). Abbreviation: MRSA, *methicillin-resistant Staphylococcus aureus.*

A time-kill experiment was next performed to determine the mode of action of complexes **1**-**3**, **(Fig 6)**. The bacterial strains were grown for 24 hours in the presence of two different concentrations of the iron complexes. The treated bacterial suspensions were then sampled every 2 hours. In addition, a control culture without antimicrobials was set up and sampled at the same time as the treated one. A Miles and Misra experiment was then carried out to determine viability of the cell suspension.[28] The three compounds caused a more than three times log reduction of the CFU/mL at the 1xMBC concentration. At lower concentrations, all three compounds also caused a reduction of the CFU/ml, but to a lower extent than that observed in the 1xMBC experiment. Similarly, of the three iron-halide compounds, complex **2** showed the highest reduction in growth rate at the lowest tested concentration.
The integrity of the cell membrane was assessed by quantifying the amount of eDNA present in the treated and non-treated bacterial cells. It was expected that a disrupted cell membrane would lead to increased leakage of bacteria DNA. Results of this experiment revealed a substantial increase in the amount of DNA released by compound-treated cells compared to the untreated cells **(Fig 7)**.

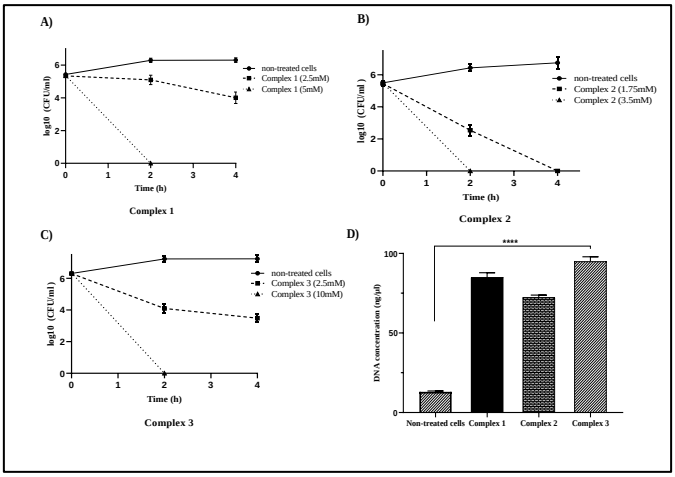


**Figure 6.** Bactericidal mode of action of the iron-halide complexes. **A, B** and **C:** Time Kill experiment - the bacteria strains were co-incubated with different concentration of the iron complexes at 37˚C. Samples were collected every two hours, serially diluted and spread on MHA plates. After 16 h at 37˚C, the plates were counted for surviving bacteria. **D)** DNA release study: cell culture containing the bacteria strains co-incubated with the iron complexes at 37˚C were centrifuged. Data represent three independent measurements (means ± SEM).

### Anti-biofilm activities of the iron-halide complexes

It is well known that biofilm formation is a mechanism that protects bacteria against antimicrobial agents. The delayed penetration of the antimicrobial agents into the biofilm matrix and its associated physiological changes have been proposed to explain this phenomenon of antibiotic resistance.[29] Therefore, it is vital to design or screen anti-biofilm molecules that can effectively inhibit and/or disperse biofilms. Herein, we first carried out a crystal violet experiment to assess the ability to prevent biofilm of the novel iron compounds. A MRSA culture was first grown in the absence and presence of different concentrations of the compounds. Crystal violet staining of the attached cells was then performed to determine the amount of biofilm formed. Results of this experiment revealed significant decrease of biofilm formation when the bacterial cultures were exposed to the each of the iron

complexes (**Fig 7**). The observed average reduction in biofilm formation was 24%, 90% and 15% for complex **2**, complex **1** and complex **3**, respectively. It is worth highlighting that this reduction in biofilm formation was also observed at concentrations of the compounds that were below the MBC values. This experimental finding suggests that the compounds specifically interfere with the molecular mechanisms that promote biofilm formation.
In a parallel experiment, biofilm-dispersal ability of the iron complexes was also studied. The pre-formed biofilms of the MRSA strain were exposed to different concentrations of the iron compounds (values ≤ MBC). As a control experiment, pre-formed biofilms were also exposed to a compound-free medium. After 24 h post-incubation, crystal violet staining was carried out to evaluate biofilm reduction. The results showed an 80 % biofilm reduction with complexes **1** and **2**, in contrast to the average 25% reduction observed with complex **3 (Fig 7)**. Like the prevention experiment, the dispersal activity of the compound was observed at concentrations of the compounds that were above and below the MBC values.

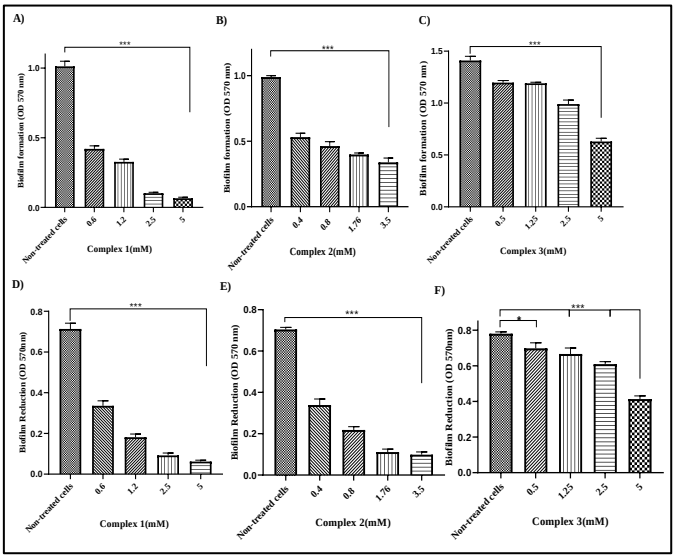


**Figure 7:** Anti-biofilm activity of the iron-halide complexes. **A)**, **B)** and **C):** Prevention of bacteria biofilm- the MRSA strains grown in a 96-wells plate was co-incubated with different concentrations of the iron complexes at 37˚C for 24 hours. Crystal violet staining of the cells attached to the bottom of the plate was followed by solubilisation of the dye and optical density measurement at 570 nm. **D)**, **E)** and **F):** Biofilm dispersal - pre-formed biofilms of the MRSA strain were incubated at 37˚C for 24 hours with RPMI media containing different concentrations of the iron-halide compounds (≤ MBC). Removal of the medium was then followed by crystal violet staining, dye solubilisation and optical density measurement at 570nm. Data were analysed statistically by one-way ANOVA. The graph represents the average absorbance of the crystal violet-stained biofilms formed on microtiter well plates. ** P<0.001 versus control

**Effect of the iron complexes on the viability and proliferation of mammalian cells (HaCaT)**

The MTT reduction assay was first used to study the *in vitro* effects of the iron complexes on the viability of the HaCaT cell line (**Fig 8**). Cells exposed to concentrations from 5 mM to 30 mM of complexes 1 and 2 exhibited a significant decrease in the MTT reduction after 24 h exposure (approx. 25 -75% inhibition of control values; $p<0.005$). No significant reduction of cell viability was observed in the cells treated with lower concentrations (< 5 mM) of complexes **1** and **2**. However, the keratinocyte cells exposed to concentrations from 0.2-30 mM of complex **3** showed significant decrease in the level of MTT reduction.
The results of the Alamar Blue assay coincided with the experimental findings shown by the MTT reduction study (**Fig 8**). Although, complex **2** caused a more substantial reduction of the metabolic activity than the tetrachloride. Similarly, the Alamar Blue assay showed that among the three iron-halide compounds, complex **3** caused the most significant reduction of metabolic activity. An Alamar Blue assay performed on neural cells also revealed complex **3** caused the largest reduction of survival cells (**Fig S3**).
A Trypan Blue assay was performed to investigate the effect of the iron-halide complexes on cell proliferation. Figure S4 shows that both complex **1** and **3** only caused significant reduction of survival cells at 5 mM concentration. However, cells treated with complex 2 exhibited important reduction of the survival cells at concentration lower than 5 mM (**Fig S4**).
The toxic effects of iron complexes on the cell line was further compared in terms of their $IC_{50}$ values, which is the concentration required to decrease the level of MTT reduction by 50% compared to the non-exposed control. An $IC_{50}$ value at 24 h was estimated at 15 mM, 7.5 mM and 1 mM for complex **1**, complex **2** and complex **3** respectively (**Fig 9**).

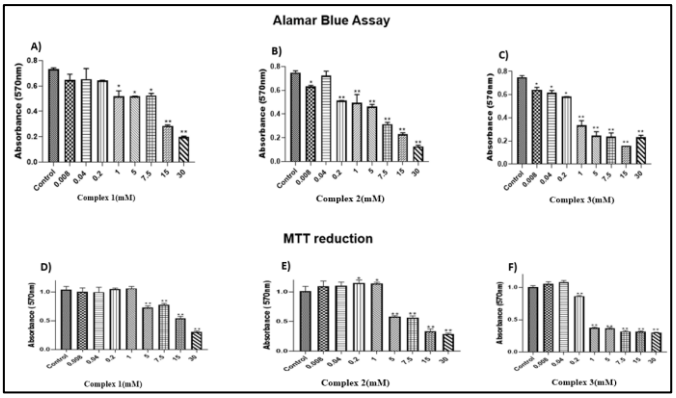


**Figure 8:** Effects of iron-halide compounds on cultured HaCaT (keratinocyte) cell viability. Cells were seeded in 96-well plates at a density of 25,000 cells/ ml and after 24 h recovery, they were treated with (0.08-30 mM) or without the iron-halide complexes, **1**, **2** and **3** (Control), for 24 h. Cell viability was measured by MTT reduction and Alamar Blue assays. Data represents means of three independent experiments ± SEM. Asterisks * indicate $p < 0.05$.

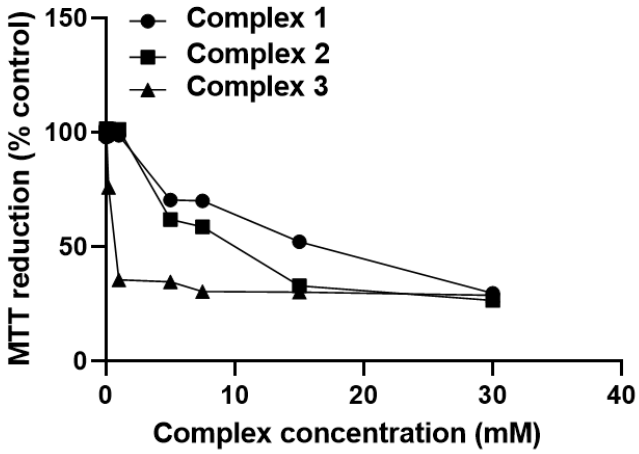


**Figure 9:** Effects of iron-halide compounds on cultured keratinocyte cell viability measured by MTT reduction. Cells were incubated in the absence (0) or presence of 0.08-30 mM complex **1**, **2** and **3** for 24 h, and cell viability assessed by MTT reduction assays as described in the experimental section. Data represent means of three independent experiments ± SEM and the results are presented as percentage relative to the corresponding control (=100%)

## Conclusions

Antimicrobial resistance is a real threat to global health with multidrug-resistant microorganisms causing millions of deaths every year.[1,30] The problem is aggravated by the fact that in the past years, there has been a significant decline in the research and development of new antibiotics.[31] As a result of this, the treatment of infectious diseases caused by multi-drug resistant microbes presents a fundamental and challenging problem. To overcome this challenge, several research groups aim to discover novel antibiotic compounds with mechanisms of action that are unknown to the pathogenic bacteria.[32] Herein, we investigated the antimicrobial activity of three novel iron complexes against a group of antibiotic-resistant strains of Gram-positive and Gram-negative bacteria.

The results of the well diffusion test demonstrated that complexes **1**-**3** and their $FeCl_3$ and $FeBr_3$ precursor salts have a broad-spectrum antimicrobial activity, as they inhibited the growth of Gram-positive and Gram-negative bacterial strains. This observation, and further determination of the MBC, validated the conclusion that the novel iron compounds retain the antimicrobial activity of their ligand.

Both, complexes **1** and **3** have higher antimicrobial activity than their ligand, as shown by their lower MBC values. It is worth highlighting that the MBC of the complex 3 is approximately twice that of the one observed with the complex 1. This finding suggests a potential role of the chloride moiety in the antimicrobial mechanism of the compounds.

The complex **2** exhibited the lowest MBC values among the three iron complexes. This result also suggests a central role of the halide moiety in the antimicrobial mechanisms, since all of these complexes differ in the type or number of halogen atoms. Moreover, it is worth highlighting that among the three iron-halide complexes only the complex **1** and **3** acted as more potent antibacterial agents than the $FeCl_3$ metal precursor. This experimental finding

correlates with the enhanced antimicrobial activity of metal complexes reported by others.[33,34] The authors of these studies suggested that the increased antimicrobial effect of the new complexes could be caused by a more efficient diffusion of the metal complexes into and/or interaction with the bacterial cell.

The observed inhibition of the bacterial cell growth by the iron-halide complexes and their ligand is also consistent with studies that reported the use of halogens and halogen-releasing gents as antimicrobial agents. For instance, Stoimenov *et al.* reported that treating nanoparticles (NPs) with halogens can increase their antibacterial activity.[35] These modified NPs were equally active against both Gram-negative and Gram-positive bacteria. The authors concluded that the high activity was caused by the abrasiveness, high surface area, and oxidizing power of the halogens.

Results of the time-kill assay demonstrated a bactericidal mode of action of the novel iron complexes, as they caused at least a three times log reduction in the CFU/ml. These iron (II/III) compounds act on bacterial cell growth in a dose-response manner, as the killing rate was higher in the cultures treated with MBC than the one exposed to 50% MBC. The experiment also showed that among the three iron complexes, complex **2** followed by complex **1** exhibited the highest killing rate. This result is consistent with the highest antimicrobial activity shown these tetra-halogenated compounds in the MBC experiment.

We also quantified the amount of extracellular DNA to evaluate whether the cell death induced by the iron complexes was associated with leakage of intracellular components. The study demonstrated an increase in the release of extracellular DNA upon exposure to the iron complexes and therefore validated a bacteriolytic mode of action. This bactericidal activity of the iron-halide complexes correlated with those studies reporting bacteriolytic activity of chlorine-releasing agents and metal-halide.[36,37]

The effect of the iron-halide complexes on biofilm prevention and dispersal was also investigated. The three complexes showed anti-biofilm activity, but the strongest reductions were observed with complexes **1** and **2**. This anti-biofilm activity was observed even at sub-lethal concentrations of the compounds, which strongly suggests that the halogenated iron compounds have the ability to interfere with the molecular mechanisms underlying biofilm formation and dispersal. These experimental findings are consistent with what Lellouche *et al.* reported in terms of anti-biofilm activity of halogenated derivatives.[38] The authors of this study observed the inhibition of *E. coli* and *S. aureus* biofilms by $MgF_2$-covered nanomaterials.

The data obtained from the viability assays in the present study have demonstrated that the iron-halide compounds are cytotoxic to the keratinocyte and neuronal cell lines in a concentration-dependent manner. The MTT reduction test and the Alamar Blue assay revealed the complex **3** as the most toxic compound for both keratinocyte and neural cells. This result strongly suggests that the metabolic effects of the 3 compounds are not mammalian cell-type specific. Therefore, similar toxicity mechanisms are likely to occur in different cell types.

We also explored the question of whether the iron-halide complexes exert any cytotoxic effect against mammalian cells at concentrations that show antimicrobial activity. The toxicity of complex **1** to the keratinocyte cell line was exhibited at higher concentrations than those at which this compound showed anti-biofilm properties. Comparable results were observed in MTT reduction and Trypan Blue assays of keratinocyte cells treated with complex **2**. However, the Alamar Blue assay of the complex **2**-treated cells showed mammalian cell toxicity at lower concentrations than those inhibiting biofilm formation. Similarly, complex **3** triggered toxicity in the keratinocyte cell line at concentrations lower than those with anti-biofilm activity. The moderately high mammalian toxicity exhibited by complex **3** could hinder its potential commercial use.

Taken together, the microbiology and cytotoxicity studies demonstrated that both complex **1** and complex **2** compounds have the potential to be efficient antibacterial agents. Further studies will be focused on improving the antimicrobial activity of those iron-halide compounds as well as reduction of toxicity to mammalian cells. To address this challenge, nanoparticles will be utilised as a carrier for the delivery of the iron-halide complexes. It has been shown that combinatorial nanoparticle systems could not only enhance antimicrobial activity, but also prevent mammalian cell toxicity.[39,40]

## Notes

Crystallographic Data for complex **2** and **3** can be found at the CCDC data base 1983590 and 1953591, respectively.

## Conflicts of interest

There are no conflicts to declare

## Acknowledgements

The authors gratefully acknowledge Bangabandhu Science and Technology Fellowship Trust', Bangladesh, and Bangladesh Council of Scientific and Industrial Research (BCSIR), Bangladesh for awarding fellowship to NA and supporting the study. AJC, AJF and FDC also acknowledge School of Science and Technology, Nottingham Trent University, UK for financial support and necessary research facilities

## References

1 D. Jasovský, J. Littmann, A. Zorzet and O. Cars, *Ups. J. Med. Sci.*, 2016, **121**, 159–164.
2 A. Taylor, J. Littmann, A. Holzscheiter, M. Voss, L. Wieler and T. Eckmanns, *Lancet*, 2019, **394**, 2050–2051.
3 J. M. Munita and C. A. Arias, *Microbiol. Spectr.*, 2016, **4**, VMBF-0016-2015.
4 *Antibiotic resistance threats in the United States, 2019*, Centers for Disease Control and Prevention (U.S.), 2019.
5 E. Gerits, E. Blommaert, A. Lippell, A. J. O'Neill, B. Weytjens, D. De Maeyer, A. C. Fierro, K. Marchal, A. Marchand, P. Chaltin, P. Spincemaille, K. De Brucker, K. Thevissen, B. P. A. Cammue, T. Swings, V. Liebens, M. Fauvart, N. Verstraeten and J. Michiels, *PLoS One*, 2016, **11**, e0155139–e0155139.
6 S. L. Solomon and K. B. Oliver, *Am. Fam. Physician*, 2014, 89, 938.
7 N. Singh and V. Manchanda, *Clin. Microbiol. Infect.*, 2017, **23**, 216–218.
8 G. M. Rossolini, E. Mantengoli, J.-D. Docquier and R. A. Musmanno, *Epidemiology of infections caused by multiresistant Gram-negatives: ESBLs, MBLs, panresistant strains*, 2007, vol. 30.
9 D. Oduro-Mensah, N. Obeng-Nkrumah, E. Y. Bonney, E. Oduro-Mensah, K. Twum-Danso, Y. D. Osei and S. T. Sackey, *Ann. Clin. Microbiol. Antimicrob.*, 2016, **15**, 29.
10 G. Sganga, *J. Med. Microbiol. Diagnosis*, 2014, **03**, 1–6.
11 E. Peterson and P. Kaur, *Front. Microbiol.*, 2018, **9**, 2928.
12 E. Yousif, A. Majeed, K. Al-Sammarrae, N. Salih, J. Salimon and B. Abdullah, *Arab. J. Chem.*, 2017, **10**, S1639–S1644.
13 M. Sunitha, P. Jogi, B. Ushaiah and C. G. Kumari, *E-Journal Chem.*, 2012, **9**, 2516–2523.
14 M. L. Beeton, J. R. Aldrich-Wright and A. Bolhuis, *J. Inorg. Biochem.*, 2014, **140**, 167–172.
15 N. K. Chaudhary and P. Mishra, *Bioinorg. Chem. Appl.*, 2017, **2017**, 6927675.
16 M. A. Malik, O. A. Dar, P. Gull, M. Y. Wani and A. A. Hashmi, *Medchemcomm*, 2018, 9, 409–436.
17 J. R. Anacona and C. Toledo, *Transit. Met. Chem.*, 2001, **26**, 228–231.
18 A. F. Santos, D. F. Brotto, L. R. V Favarin, N. A. Cabeza, G. R. Andrade, M. Batistote, A. A. Cavalheiro, A. Neves, D. C. M. Rodrigues and A. dos Anjos, *Rev. Bras. Farmacogn.*, 2014, **24**, 309–315.
19 W. Guerra, E. De Andrade Azevedo, A. R. De Souza Monteiro, M. Bucciarelli-Rodriguez, E. Chartone-Souza, A. M. A. Nascimento, A. P. S. Fontes, L. Le Moyec and E. C. Pereira-Maia, *J. Inorg. Biochem.*, 2005, **99**, 2348–2354.
20 M. Aldabaldetrecu, L. Tamayo, R. Alarcon, M. Walter, E. Salas-Huenuleo, M. J. Kogan, J. Guerrero, M. Paez and M. I. Azócar, *Molecules*, 2018, **23**, 1629.
21 K. Gałczyńska, K. Ciepluch, Ł. Madej, K. Kurdziel, B. Maciejewska, Z. Drulis-Kawa, A. Węgierek-Ciuk, A. Lankoff and M. Arabski, *Sci. Rep.*, 2019, **9**, 9777.
22 E. K. Rusbridge, Y. Peng, A. K. Powell, D. Robinson and A. J. Fitzpatrick, *Dalt. Trans.*, 2018, **47**, 7644–7648.
23 B. L. Z. Jean B. Patel, Franklin R. Cockerill III, Jeff Alder, Patricia A. Bradford, George M. Eliopoulos, MD Dwight J. Hardy, Janet A. Hindler, Stephen G. Jenkins, James S. Lewis II, PharmD Linda A. Miller, Mair Powell, Jana M. Swenson, Maria M. Traczewski, John, *Performance Standards for Antimicrobial Susceptibility Testing; Twenty-Fourth Informational Supplement (M100-S24)*, 2014.
24 R. D. Fields and M. V. Lancaster, *Am. Biotechnol. Lab.*, 1993, **11**, 48–50.
25 S. Ansar Ahmed, R. M. Gogal and J. E. Walsh, *J. Immunol. Methods*, 1994, **170**, 211–224.
26 T. Mosmann, *J. Immunol. Methods*, 1983, **65**, 55–63.
27 R. I. Freshney, in *Culture of Animal Cells*, John Wiley & Sons, Inc., 2005.
28 A. A. Miles, S. S. Misra and J. O. Irwin, *J. Hyg. (Lond).*, 1938, **38**, 732–749.
29 H. Koo, R. N. Allan, R. P. Howlin, P. Stoodley and L. Hall-Stoodley, *Nat. Rev. Microbiol.*, 2017, **15**, 740–755.
30 A. Tagliabue and R. Rappuoli, *Front. Immunol.*, 2018, **9**, 1068.
31 E. Tacconelli, E. Carrara, A. Savoldi, S. Harbarth, M. Mendelson, D. L. Monnet, C. Pulcini, G. Kahlmeter, J. Kluytmans, Y. Carmeli, M. Ouellette, K. Outterson, J. Patel, M. Cavaleri, E. M. Cox, C. R. Houchens, M. L. Grayson, P. Hansen, N. Singh, U. Theuretzbacher, N. Magrini, A. O. Aboderin, S. S. Al-Abri, N. Awang Jalil, N. Benzonana, S. Bhattacharya, A. J. Brink, F. R. Burkert, O. Cars, G. Cornaglia, O. J. Dyar, A. W. Friedrich, A. C. Gales, S. Gandra, C. G. Giske, D. A. Goff, H. Goossens, T. Gottlieb, M. Guzman Blanco, W. Hryniewicz, D. Kattula, T. Jinks, S. S. Kanj, L. Kerr, M.-P. Kieny, Y. S. Kim, R. S. Kozlov, J. Labarca, R. Laxminarayan, K. Leder, L. Leibovici, G. Levy-Hara, J. Littman, S. Malhotra-Kumar, V. Manchanda, L. Moja, B. Ndoye, A. Pan, D. L. Paterson, M. Paul, H. Qiu, P. Ramon-Pardo, J. Rodríguez-Baño, M. Sanguinetti, S. Sengupta, M. Sharland, M. Si-Mehand, L. L. Silver, W. Song, M. Steinbakk, J.

Thomsen, G. E. Thwaites, J. W. M. van der Meer, N. Van Kinh, S. Vega, M. V. Villegas, A. Wechsler-Fördös, H. F. L. Wertheim, E. Wesangula, N. Woodford, F. O. Yilmaz and A. Zorzet, *Lancet Infect. Dis.*, 2018, **18**, 318–327.
32 E. Banin, D. Hughes and O. P. Kuipers, *FEMS Microbiol. Rev.*, 2017, **41**, 450–452.
33 K. Singh, *J. Enzyme Inhib. Med. Chem.*, 2006, **21**, 557–562.
34 Z. H. Chohan, Mahmood-ul-Hassan, K. M. Khan and C. T. Supuran, *J. Enzyme Inhib. Med. Chem.*, 2005, **20**, 183–188.
35 P. K. Stoimenov, R. L. Klinger, G. L. Marchin and K. J. Klabunde, *Langmuir*, 2002, **18**, 6679–6686.
36 A. D. Russell, *J. Antimicrob. Chemother.*, 2003, **52**, 750–763.
37 V. Sambhy, M. M. MacBride, B. R. Peterson and A. Sen, *J. Am. Chem. Soc.*, 2006, **128**, 9798–9808.
38 J. Lellouche, A. Friedman, R. Lahmi, A. Gedanken and E. Banin, *Int. J. Nanomedicine*, 2012, **7**, 1175–1188.
39 O. Choi, K. K. Deng, N.-J. Kim, L. Ross, R. Y. Surampalli and Z. Hu, *Water Res.*, 2008, **42**, 3066–3074.
40 J. F. A. de Oliveira, Â. Saito, A. T. Bido, J. Kobarg, H. K. Stassen and M. B. Cardoso, *Sci. Rep.*, 2017, **7**, 1326.